Journal of Materials Chemistry A

Accepted Manuscript

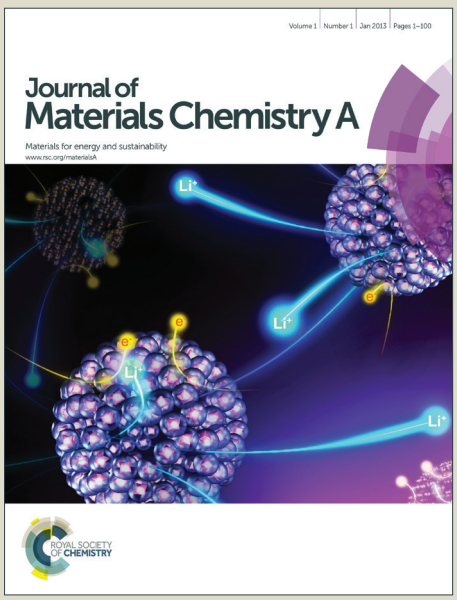

ROYAL SOCIETY OF CHEMISTRY

www.rsc.org/materialsA

Design of tetraphenyl silsesquioxane based covalent-organic frameworks as hydrogen storage materials

Xiao-Dong Li,[*1] Hua-Ping Zang,[2] Jun-Tao Wang,[1] Jun-Fei Wang[1] and Hong Zhang[*3]

[1]*College of Science, Henan University of Technology, Zhengzhou 450001, China*

[2]*School of Physics and Engineering, Zhengzhou University, Zhengzhou, Henan 450001, China*

[3]*College of Physical Science and Technology, Sichuan University, Chengdu 610065, China*

Abstract

Four types of tetraphenyl silsesquioxane based covalent-organic frameworks (sil-COFs) were designed with the ctn and bor net topologies using the molecular mechanics. The computed results reveal that these sil-COFs possess excellent structural properties such as high porosity (89% - 95%) and large H_2 accessible surface area (5476 - 6331 m^2/g), which is advantageous to hydrogen storage. The H_2 adsorption isotherms of these sil-COFs were simulated with the method of grand canonical Monte Carlo (GCMC) at 77 K and 298 K. The simulated results indicate that at 77 K the sil-COF-4 has the highest gravimetric hydrogen storage capacity of 36.82 wt% while the sil-COF-1 owns the highest volumetric hydrogen storage capacity of 63.53 g/L. At 298 K, the sil-COF-4 has the highest gravimetric hydrogen uptake of 5.50 wt%, which already exceeds the U.S. Department of Energy's goal (4.5 wt%) for 2017 and are also very close to the criterion of 6 wt% for practical application of hydrogen at room temperature. In addition, two possible schemes are proposed to synthesize the sil-COFs.

[*]Authors to whom correspondence should be addressed, E-mail: xiaodonglihaut@163.com and hongzhang@scu.edu.cn

Keywords: sil-COF, tetraphenyl silsesquioxane, hydrogen adsorption, grand canonical Monte Carlo

Introduction

The safe and effective storage of hydrogen is one of the main problems obstructing hydrogen as widely used energy carrier in the system of hydrogen energy.[1, 2] During the past years, porous materials based hydrogen storage[3-5] has been considered as one of the most promising methods for practical application. Many porous materials, such as metal-organic frameworks (MOFs),[6-8] covalent-organic frameworks (COFs),[9-12] porous aromatic frameworks (PAFs),[13, 14] and so on, have been proposed as hydrogen storage media. Among these materials, COFs are one type of porous crystalline materials with two-dimension (2D) or three-dimension (3D) structures constructed by strong covalent bonds between the light elements such as C, H, O, B and Si.[9, 15] COFs have the large porous volume, the high surface area and the extremely low density, which are advantage to gas storage and separation. Therefore, many studies including experiments and theories[10, 16-21] have been performed to study the hydrogen storage properties of COFs and their modified counterparts.

Furukawa and Yaghi measured the H_2 adsorption isotherms on a series of COFs at the pressure of 1-85 bar and the temperature of 77 -298 K in experiment.[20] They well described the H_2 uptake behavior and capacity of these COFs by classifying them into three groups based on their structural dimensions and corresponding pore sizes. Xiang et al, first synthesized a covalent-organic polymer in experiment and then they proposed a novel lithium-decorating approach to enhance its H_2 adsorption properties.[21] Surprisingly, the H_2

uptake of lithium-modified material is increased by 70.4%, compared with the unmodified compounds. With the method of GCMC simulations, Garberoglio obtained the hydrogen adsorption isotherms of several 3D-COFs.[22] The results show that these COFs might attain a 30% increase for the uptake when compared with analogous simulations performed for MOFs at 77 K and 298 K. By combining first-principles calculations and GCMC simulations, Cao et al, studied the hydrogen storage capacities of lithium-doped 3D-COFs.[23] The simulations demonstrate that gravimetric adsorption capacities for hydrogen in Li-doped COF-105 and COF-108 can reach 6.84 wt% and 6.73 wt% at 298 K and 100 bar, which have met the requirements for practical use in hydrogen storage. Also, Mendoza-Cortes performed systematic investigations on hydrogen storage in several COFs and their Li- , Na-, and K-metalated systems.[18] In addition, Li et al, proposed a way of promoting the binding of H_2 on COFs crystals via substituting the bridge C_2O_2B rings with different metal-participated rings.[24] With this method, the H_2 binding energy can achieve 10 kJ/mol enhanced by a factor of four with regard to the undoped crystal. All these studies indicate the potential of COFs as practical hydrogen storage materials.

Besides the experimentally synthesized COFs or their modified counterparts, many novel COFs have been designed as hydrogen storage materials in theory as well.[25-29] Klontzas designed four types of 3D-COFs with enhanced hydrogen storage capacity.[29] The simulations demonstrate that their maximum gravimetric H_2 uptake can overpass 25 wt% at 77 K and reach the Department of Energy's target of 6 wt% in room temperature. Using the similar method, Mendoza-Cortes designed 14 new COFs, which can adsorb large amounts of methane at 298 K and up to 300 bar.[28] Also, by inserting the pyridine molecules into the

2D-COF-1 layers, Kim et al. proposed several pillared COFs (PCOFs) to expose the buried framework surfaces to pores.[27] With this approach, the PCOFs have significantly improved gravimetric and volumetric hydrogen storage capacities of 8.8-10.0 wt% and 58.7-61.7 g L^{-1}, respectively. All these experiences provide valuable references for synthesizing new COFs with excellent hydrogen storage properties in future.

Silsesquioxane is one type of compounds with inerratic geometry structures capable of forming nanocomposites.[30, 31] They are nanoscopic cages in size and are comprised of rigid 3D Si-O frameworks with the form of $(RSiO_{3/2})_n$, (n = 4, 6, 8, ...), where R can be typically an alkyl or an aryl organic group, etc.[32, 33] The organic groups of silsesquioxanes can be made reactive for polymerization, and hence they are very promising building blocks for constructing porous materials.[33-35] Not long ago, some researchers have reported several octahedral silsesquioxane ($R_8Si_8O_{12}$) based porous materials with specific net topology.[36-39] The tetrahedral silsesquioxane ($R_4Si_4O_6$) is the simplest silsesquioxane, and thus it has the potential to build low-density porous materials. To the best knowledge, there is no related report on the tetrahedral silsesquioxane based porous materials in experiment up to now. Herein, we propose four covalent-organic frameworks based on tetraphenyl silsesquioxane as hydrogen storage materials in present work. The computations reveal that the designed sil-COFs have high porosities, large surface areas and very low densities. The H_2 adsorption isotherms obtained by GCMC simulations demonstrate the excellent hydrogen storage capacities of these sil-COFs. The suitable structural properties and the high hydrogen storage capacities indicate the potential use of sil-COFs as hydrogen storage media.

Design and computation details

For the design of 3,4 frameworks, the ctn (a hypothetical C_3N_4 structure, $I\bar{4}3m$ space group) and bor (boracite, $P\bar{4}3m$ space group) net structures are considered to be the most stable two.[11, 28, 40] The reported 3D-COFs such as COF-102, COF-103, COF-105 and COF-108 do all belong to these two topologies.[11] Conceptually, by replacing the triangular and tetrahedral sites in ctn and bor net frameworks with suitable building units, two types of framework materials can be obtained. Therefore, in this study, we select tetraphenyl silsesquioxane and two types of triangular units as building units to assemble framework materials with ctn or bor net topologies. The geometry structures of these building units are shown in Fig. 1. The potential of tetraphenyl silsesquioxane as building unit has been discussed in previous part and the two triangular units are the main building units of existing 3D-COFs.[11] Based on these building units, four types of tetraphenyl silsesquioxane based covalent-organic frameworks (sil-COFs) are obtained and the designed schemes are depicted in Fig. 1. Here we term the four sil-COFs as sil-COF-1, sil-COF-2, sil-COF-3, and sil-COF-4 for convenience.

Insert Figure 1

Before constructing the sil-COFs, we first optimized three building units using generalized gradient approximation within the framework of density function theory. Then we assembled the four sil-COFs by adding the irreducible representations of the ligands into the topological structures with the corresponding space groups. During the process, none of

the building units produce the lower symmetry. Here the sil-COF-1 and sil-COF-3 (sil-COF-2 and sil-COF-4) follow $I\bar{4}3m$ ($P\bar{4}3m$) space group symmetry, while the sil-COF-1 and sil-COF-2 (sil-COF-3 and sil-COF-4) are comprised of the same building units, as shown in Fig. 1. Based on the preliminary design, we subsequently optimized the sil-COFs with the classical molecular mechanics method with the molecular mechanics method with Dreding force field.[41] During the optimized process, the conjugate gradient method was designed to begin with steepest descent method as the first step. To get the best structures, no space group symmetry constrains were imposed on the frameworks and all the bond lengths, angles, and cell parameters were well optimized. The geometries are optimized until the remaining atomic forces are less than 0.0001 kcal/(mol·Å) on each atom and the energy convergence criterion is chosen as 1.0×10^{-5} kcal/mol between two steps.

On the basis of the optimized structures, the H_2 adsorption isotherms of these sil-COFs were computed by GCMC simulations. The Van der Waals interactions between the H_2 molecule and the frameworks were treated as 12-6 Lennard-Jones (LJ) potential as shown in equation (1). The LJ potential parameters of the framework atoms were taken from the Dreding force field of Mayo et al,[41] and the potential parameters of H_2 molecules were from the work of Buch[42] where a united-atom model was employed. All the potential parameters used in the present work are presented in Table 1. The cross-interaction parameters between different types of atoms were calculated using the Lorentz–Berthelot mixing rules shown in equation (2) and (3). In addition, the LJ interactions were calculated with a spherical cut-off value of 13 Å.

$$U_{LJ} = -4\varepsilon_{ij}[(\frac{\sigma_{ij}}{r_{ij}})^6 - (\frac{\sigma_{ij}}{r_{ij}})^{12}] \qquad (1)$$

$$\sigma_{ij} = (\sigma_{ii} + \sigma_{jj})/2 \quad (2)$$

$$\varepsilon_{ij} = \sqrt{\varepsilon_{ii}\varepsilon_{jj}} \quad (3)$$

The GCMC simulations were carried out using the code Music.[43] The input fugacities for H_2 gas were calculated by Peng-Robinson equation of state (P-R EOS).[44] During the simulations, the $2\times2\times2$ supercells for all sil-COFs were adopted and the periodic conditions were applied on all three dimensions. The frameworks were frozen during the simulations. A typical GCMC simulation point included a total of 2×10^7 Monte Carlo steps. The first 1×10^7 steps were used for equilibration and the subsequent 1×10^7 steps were used for ensemble average. Each Monte Carlo step was consisted of three trivial moves for H_2 molecules, namely, insertion of a new molecule, deletion of an existing molecule, or translation of an existing molecule. In addition, the excess H_2 adsorption amounts (N_{exc}) were calculated by equation (4)

$$N_{exc} = N_{abs} - \rho V_p \quad (4)$$

Here, N_{abs} is the absolute H_2 adsorption amounts, ρ refers the density of H_2 gas under the thermodynamics conditions studied, and V_p denotes the pore volume of the adsorbent. The density of H_2 gas under a given pressure and temperature was computed by P-R EOS.[44] The pore volumes of these sil-COFs were evaluated with the method of Talu and Myers.[45] They proposed that the pore volume of a porous material could be estimated by the amounts of helium molecules (N_a) adsorbed at low pressure (P) and room temperature (T_0) with equation (5)

$$V_p = N_a K_B T_0 / P \quad (5)$$

where K_B is the Boltzmann constant. The veracity of the employed force field parameters and

the simulation method were validated in our previous paper.[46]

Additionally, the isosteric heat of adsorption for H_2 molecule (Q_{st}) was calculated with equation (6)[47]

$$Q_{st} = RT - \left(\frac{\partial \langle v \rangle}{\partial \langle N \rangle} \right)_T \qquad (6)$$

Here, R denotes the ideal gas constant, T is the temperature, v represents potential energy of the adsorbed phase, N is the number of molecules in the adsorbed phase, and the angular brackets indicate an ensemble average.

Insert Table 1

Results and discussions

Based on the geometry optimization, the final structures of four sil-COFs are obtained. The results reflects that all four sil-COFs maintain the same space group symmetries as the initial designed ones under the tolerance of 10^{-5} Å. The cell and physical parameters for the periodic sil-COF structures are listed in Table 2. The space group symmetries and coordinates of these sil-COF frameworks are provided in the supporting information. Seeing the results in Table 2, we can find that the cell length for four sil-COFs follows the sequence of sil-COF-2 < sil-COF-4 < sil-COF-1 < sil-COF-3. sil-COF-1 (sil-COF-3) has the larger unit cell length than that of sil-COF-2 (sil-COF-4), although they are consisted of the same building blocks. This is ascribed to the different topological structures of these sil-COFs. On the other hand, as the triangular building units in the sil-COF-3 and sil-COF-4 are larger that of sil-COF-1 and sil-COF-2, sil-COF-3 (sil-COF-4) has much larger unit cell length than that of sil-COF-1

(sil-COF-2) although they have the same topological structure. It can be seen in Table 2 that all sil-COFs have very low densities (0.15-0.33 g/cm^3). To our knowledge, the experimentally reported COFs with the lowest density are COF-108 (0.17 g/cm^3) and COF-105 (0.18 g/cm^3).[11, 23] Impressively, sil-COF-3 and sil-COF-4 own even lower density than COF-105 and COF-108, which reflects that they have entered the lists of porous materials with the lowest density.

Insert Table 2

The pore size and the surface area are two important indexes to judge the gas adsorption capacity of porous materials. The pore volumes of four sil-COFs were calculated by the amounts of helium molecules adsorbed at the temperature of 298 K and the pressure of 0-1 bar. As seen in Table 2, the pore volume of four sil-COFs follows the sequence of sil-COF-1 < sil-COF-2 < sil-COF-3 < sil-COF-4, which is just opposite to the sequence of density. To get a concrete concept of the pore size, the percent pore volumes of four sil-COFs are also estimated and they are 89%, 90%, 94% and 95% for sil-COF-1 to sil-COF-4, respectively. To the best of our knowledge, the percent pore volumes of COF-105 (88.22%), COF-108 (88.84%) and PAF-1 (77.60%)[11, 23, 48] are the highest ones reported for porous materials in experiment. Surprisingly, the percent pore volume of these sil-COFs has exceeded the porous materials with the highest porosity up to now. Also, we evaluated the surface areas of these sil-COFs by the accessible surface area. The accessible surface areas were calculated by using a numerical Monte Carlo integration technique proposed by Frost et al.[49] It was performed by

"rolling" a spherical probe H_2 molecule with a diameter equal to the LJ σ parameter of H_2 molecule (2.958 Å). The probe was inserted randomly around the surface of each framework atom with a diameter equal to the LJ σ parameters one by one. The fraction of probes that did not overlap with other framework atoms was used to calculate the accessible surface area. It is clear that the accessible surface area is highly dependent on the probe size used for measurement, and calculating the surface area using a H_2 probe provides the amount of area accessible to H_2 molecules. The calculated accessible H_2 surface areas for four sil-COFs are listed in Table 2. The sequence of H_2 accessible surface area for four sil-COFs is sil-COF-2 < sil-COF-1 < sil-COF-4 < sil-COF-3. It can be found that for the same two building units, the structure with ctn net topology has the larger surface area than that with bor net topology, while under the same net topology, the structure with larger triangular building units own the even larger surface area. Anyhow, all four sil-COFs have quite larger surface areas. Up to now, the highest surface area reported for MOF materials is claimed for MOF-210, which has a Brunauer–Emmett–Teller (BET) surface area of 6240 m^2/g and a Langmuir surface area of 10400 m^2/g.[50] In addition, highest surface area reported for COF materials is 4210 m^2/g (BET) in COF-103 up to now.[11] Also, PAF-1 owns a very high BET surface area of 5600 m^2/g and a Langmuir surface area of 7100 m^2/g.[48] The accessible surface areas for four sil-COFs in Table 2 reflect that all sil-COFs reported here are on a par with the porous materials with the highest surface area. Both the high porosity and the large surface area indicate that these sil-COFs will exhibit good hydrogen storage capacity.

Insert Figure 2

To validate the veracity of the employed force field based on the LJ potential model and the GCMC method, the absolute H_2 adsorption capacities of COF-102 are calculated at 77 K and the adsorption isotherms are shown in Fig. 2. The experimental data by Furukawa and Yaghi[20] and other simulated results by Han et al.[51] and Klontzas et al.[52] with different parameters are also shown in Fig. 2. As shown in Fig. 2, the trend of our simulated results is consistent with the experimental data with only a little larger. Therefore, this force field based on the LJ potential model will be utilized for further study in this work.

Insert Figure 3

The H_2 adsorption isotherms for four sil-COFs at 77 K are simulated using the GCMC method and the results are shown in Fig. 3. As can be seen in Fig. 3, the absolute gravimetric and volumetric H_2 adsorption capacities increase gradually with the rise of H_2 gas pressure from 0.1 bar to 100 bar. Other than absolute capacities, the excess H_2 adsorption capacities reach their maximum at the moderate H_2 gas pressure. Figure 2(a) shows that the H_2 gravimetric adsorption capacity of sil-COF-1 is higher than that of sil-COF-2 at $P \leq 40$ bar while it is reversed at $P > 40$ bar. On the other hand, the H_2 gravimetric adsorption capacity of sil-COF-4 is higher than that of sil-COF-3 at all the H_2 gas pressure studied. The maximum gravimetric H_2 adsorption capacities are 19.43 wt%, 20.30 wt%, 34.83 wt% and 36.82 wt% for sil-COF-1, sil-COF-2, sil-COF-3 and sil-COF-4, respectively. In addition, the excess

gravimetric H_2 adsorption capacities are 9.66 wt% at 30 bar for sil-COF-1, 11.48 wt% at 40 bar for sil-COF-2, 14.69 wt% at 60 bar for sil-COF-3 and 14.16 wt% at 70 bar for sil-COF-4. Seeing from Fig. 3(b), we can find that the absolute volumetric H_2 adsorption capacities for four sil-COFs obey the sequence of sil-COF-1 > sil-COF-2 > sil-COF-3 >sil-COF-4, which is opposite to the absolute gravimetric H_2 adsorption capacity on the whole. The maximum absolute (excess) volumetric H_2 adsorption capacities are 63.53 g/L (40.99 g/L at 40 bar), 61.00 g/L (36.34 g/L at 40 bar), 55.58 g/L (25.00 g/L at 70 bar) and 53.36 g/L (21.88 g/L at 70 bar) for sil-COF-1 to sil-COF-4, respectively. The results reveal the excellent H_2 storage capacity of these sil-COFs at 77 K.

Insert Figure 4

As the practical use of hydrogen should be at room temperature most often, we also computed the hydrogen uptake of four sil-COFs at 298 K. It can be seen from Fig. 4 that both the absolute gravimetric and volumetric H_2 adsorption capacities increase linearly with the rise of H_2 gas pressure, which is just the character of Henry's linear isotherm equation.[53, 54] The slopes of the linear isotherms are the Henry law constants. The Henry's linear isotherm equation is $n = KP$, where n is the adsorbed amount per unit weight of adsorbent (wt%), P is the adsorbate gas pressure at equilibrium (bar), and K is the Henry's law constant (wt% per bar). We have done the linear fits for the absolute gravimetric isotherms and the fitted equations are listed in Fig. 4(a), including the respective degree of linear correlation. The subscripts 1 to 4 in these equations denote the corresponding equations and degrees of linear

correlation for sil-COF-1 to sil-COF-4. The good linearity of these isotherms reveals that the H_2 uptake capacity of these sil-COFs is related to the pore volume and virtually independent of binding energy or surface area at the room temperature. As can be seen in Fig. 4(a), the gravimetric H_2 adsorption capacities of four sil-COFs do follow the same sequence with the pore volume, that is, sil-COF-1 < sil-COF-2 < sil-COF-3 < sil-COF-4. The highest absolute gravimetric (volumetric) H_2 uptake are 2.60 wt% (8.51 g/L), 2.79 wt% (8.39 g/L), 5.05 wt% (8.05 g/L), and 5.50 wt% (7.97 g/L) for sil-COF-1 to sil-COF-4, respectively. Surprisingly, the maximum gravimetric H_2 adsorption capacities for sil-COF-3 and sil-COF-4 have exceeded U.S. Department of Energy's goal (4.5 wt%) for 2017 and also very approach the capacity (6 wt%) for practical application of hydrogen at room temperature.[55] However, the absolute volumetric H_2 uptakes for sil-COFs are all very low and are close to each other at 298 K, which again indicated that the amount of hydrogen adsorbed is mainly dependent of pore volume. To improve the volumetric H_2 capacity of these sil-COFs, some modified methods such as dope or substitution can be adopted, which are being carried out in the subsequent studies. For many studies the excess H_2 adsorption capacity is always not mentioned at room temperature, since it is always very low. Here, to make the investigation comprehensively, we also present the excess H_2 adsorption capacities at room temperature. As shown in Fig. 4, the maximum excess gravimetric H_2 uptakes are almost the same (0.2 wt%) for all sil-COFs, and the volumetric H_2 capacities are located in the range of 0.6 -2 g/L.

Insert Figure 5

Using the equation (6), we computed the isosteric heats of adsorption of H_2 molecule in four sil-COFs at both 77 K and 298 K. Table 2 lists the average isosteric heat of adsorption of H_2 molecule in each sil-COF at 77 K and 298 K. Also the original data of the entire heat of adsorption at all the adsorption points is listed in Table S5 in the supporting information. It can be seen in Table 2 and Table S5 that isosteric heats of adsorption of H_2 molecule at 298 K is larger than that of 77 K for the same sil-COF. This is attributed to the fact that much more H_2 molecules can be adsorbed on the same sil-COF at 77 K than at 298 K. The H_2 molecules are mainly adsorbed near the surface of sil-COFs at 298 K, while more H_2 molecules are accommodated in the pore cavity far from the material surface at 77 K. Since the isosteric heat of adsorption of H_2 molecule mainly comes from the Van der Waals interactions between the H_2 molecules and the framework surface, it become smaller at 77 K than at 298 K. Howbeit, the isosteric heats of adsorption of H_2 molecule in these sil-COFs are all very small. Some previous work have pointed that for practical hydrogen storage application the value of isosteric heat needs to be larger than 15 kJ/mol.[2] Hence, in order to enhance the isosteric heats of adsorption of H_2 molecule in sil-COFs, some modified methods can be adopted, which has mentioned in the previous paragraph to improve the volumetric H_2 adsorption capacity at room temperature.

To understand the adsorption process of H_2 molecules in these sil-COF frameworks, we investigated their adsorption behavior at a molecular level by detecting the snapshots of four sil-COF structures with H_2 molecules adsorbed at both 77 K and 298 K. Fig. 5 typically shows the snapshots of four sil-COFs with adsorbed H_2 molecules at 77 K and 100 bar. By studying the adsorption behavior of H_2 molecules in these sil-COFs, we find that the

triangular units, especially the B_3O_3 and BC_2O_2 rings, are the preferential adsorption sites for H_2 molecules, which is consistent with the study in the previous work by ab initio calculations.[10, 52] During the process, the H_2 molecules are first adsorbed near the triangular units at low H_2 pressure. With the rising in the H_2 pressure, the H_2 molecules begin to occupy the corner sites near the tetrahedral units. Finally, the H_2 molecules accommodate the pore space far from the framework surface at high H_2 pressure.

Insert Figure 6

At last, two possible schemes to synthesize these sil-COFs are proposed and shown in Fig. 6. As depicted in Fig. 6, the tetra(4-dihydroxyborylphenyl)silsesquioxane (TBPS) is treated as tetrahedral building block (Fig. 6A) and the hexahydroxytriphenylene (HHTP) (Fig. 6B) is selected as as triangular building block. In principle, linking tetrahedra with triangles can form an infinite number of possible nets. However, analysis of previous assembly reactions suggests that the most symmetric nets are the most likely to result in an unbiased system and that those with just one kind of link will be preferred and are thus the best to target.[11] In the present case of linking tetrahedral and triangular building blocks, the only known nets meeting the above criteria are the net with ctn and bor[11, 40] topologies shown in Fig. 1. Based on these theories, the synthesis schemes R1 and R2 are proposed to synthesize these sil-COFs, as depicted in Fig. 6. As can be seen in Fig. 6, sil-COF-1 and sil-COF-2 may be synthesized by self-condensation of TBPS to form B_3O_3 rings (Fig. 6C), while sil-COF-3 or sil-COF-4 can be obtained by co-condensation of TBPS and HHTP to form C_2O_2B rings

(Fig. 6D). The use of rigid, planar triangular units, such as B_3O_3 rings, requires that rotational freedom exist at the tetrahedral nodes to form the 3D ctn and bor structures.

Conclusions

In present work, four novel 3D tetraphenyl silsesquioxane based COFs have been designed and proposed as hydrogen storage materials. The calculated results reveal that the sil-COF porous materials have high pore volume and large H_2 accessible surface area. The GCMC simulations indicate that the sil-COF-4 owns the highest gravimetric hydrogen uptake while sil-COF-2 possesses the highest volumetric hydrogen uptake at both 77 K and 298 K. The excellent hydrogen adsorption capacity of these sil-COFs forebodes their potential as hydrogen storage materials. Meanwhile, two possible schemes are also proposed to synthesize the sil-COFs. Although to realize them in experiment still needs a long way, we hope that knowledge gained from this study will motivate some inspirations for developing the corresponding experiments.

Supporting information

The space group symmetries and coordinates of four sil-COF materials are provided in the supporting information.

Acknowledgement

X.-D. Li acknowledges financial support from the Talent Introduction Fund (No. 2013BS039) and the Plan of Nature Science Fundamental Research (No. 2013JCYJ10) in Henan

University of Technology of Technology. H.-P. Zang thanks to the financial support from China Postdoctoral Science Foundation funded project (No. 2013008).

References

1. K. Mazloomi and C. Gomes, *Renewable and Sustainable Energy Reviews*, 2012, 16, 3024-3033.
2. A. W. C. van den Berg and C. O. Arean, *Chem. Commun.*, 2008, 668-681.
3. M. Bastos-Neto, C. Patzschke, M. Lange, J. Mollmer, A. Moller, S. Fichtner, C. Schrage, D. Lassig, J. Lincke, R. Staudt, H. Krautscheid and R. Glaser, *Energy & Environmental Science*, 2012, 5, 8294-8303.
4. J. Yang, A. Sudik, C. Wolverton and D. J. Siegel, *Chem. Soc. Rev.*, 2010, 39, 656-675.
5. U. Eberle, M. Felderhoff and F. Schuth, *Angewandte Chemie International Edition*, 2009, 48, 6608-6630.
6. Y. Sun, L. Wang, W. Amer, H. Yu, J. Ji, L. Huang, J. Shan and R. Tong, *J. Inorg. Organomet. Polym. Mater.*, 2013, 23, 270-285.
7. D. Zhao, D. Yuan and H.-C. Zhou, *Energy & Environmental Science*, 2008, 1, 222-235.
8. H. Li, M. Eddaoudi, M. O'Keeffe and O. M. Yaghi, *Nature*, 1999, 402, 276-279.
9. Z. Xiang and D. Cao, *Journal of Materials Chemistry A*, 2013, 1, 2691-2718.
10. E. Tylianakis, E. Klontzas and G. E. Froudakis, *Nanoscale*, 2011, 3, 856-869.
11. H. M. El-Kaderi, J. R. Hunt, J. L. Mendoza-Cortes, A. P. Cote, R. E. Taylor, M. O'Keeffe and O. M. Yaghi, *Science*, 2007, 316, 268-272.
12. A. P. Cote, A. I. Benin, N. W. Ockwig, M. O'Keeffe, A. J. Matzger and O. M. Yaghi, *Science*, 2005, 310, 1166-1170.
13. T. Ben and S. Qiu, *CrystEngComm*, 2013, 15, 17-26.
14. Y. L. Miao, H. Sun, L. Wang and Y. X. Sun, *Acta Physico-Chimica Sinica*, 2012, 28, 547-554.
15. X. Feng, X. Ding and D. Jiang, *Chem. Soc. Rev.*, 2012, 41, 6010-6022.
16. Y. Zhu, J. Zhou, J. Hu, H. Liu and Y. Hu, *Mol. Simul.*, 2012, 38, 595-603.
17. Z. Yang and D. Cao, *J. Phys. Chem. C*, 2012, 116, 12591-12598.
18. J. L. Mendoza-Cortes, S. S. Han and W. A. Goddard, *J. Phys. Chem. A*, 2012, 116, 1621-1631.
19. J. Lan, D. Cao, W. Wang and B. Smit, *ACS Nano*, 2010, 4, 4225-4237.
20. H. Furukawa and O. M. Yaghi, *J. Am. Chem. Soc.*, 2009, 131, 8875-8883.
21. Z. Xiang, D. Cao, W. Wang, W. Yang, B. Han and J. Lu, *J. Phys. Chem. C*, 2012, 116, 5974-5980.
22. G. Garberoglio, *Langmuir*, 2007, 23, 12154-12158.
23. D. Cao, J. Lan, W. Wang and B. Smit, *Angewandte Chemie International Edition*, 2009, 48, 4730-4733.
24. F. Li, J. J. Zhao, B. Johansson and L. X. Sun, *Int. J. Hydrogen Energy*, 2010, 35, 266-271.
25. S. Bureekaew and R. Schmid, *CrystEngComm*, 2013, 15, 1551-1562.
26. R. Babarao, R. Custelcean, B. P. Hay and D.-e. Jiang, *Cryst. Growth Des.*, 2012, 12, 5349-5356.
27. D. Kim, D. H. Jung, K. H. Kim, H. Guk, S. S. Han, K. Choi and S. H. Choi, *J. Phys. Chem. C*, 2012, 116, 1479-1484.
28. J. L. Mendoza-Cortes, T. A. Pascal and W. A. Goddard, *J. Phys. Chem. A*, 2011, 115, 13852-13857.

29. E. Klontzas, E. Tylianakis and G. E. Froudakis, *Nano Lett.*, 2010, 10, 452-454.
30. J. J. Schwab and J. D. Lichtenhan, *Appl. Organomet. Chem.*, 1998, 12, 707-713.
31. J. Lichtenhan, in *Polymeric Materials Encyclopedia*, ed. J. C. Salamone, CRC Press: New York, 1996, vol. 10, pp. 7768-7777.
32. R. Y. Kannan, H. J. Salacinski, P. E. Butler and A. M. Seifalian, *Acc. Chem. Res.*, 2005, 38, 879-884.
33. A. J. Waddon, L. Zheng, R. J. Farris and E. B. Coughlin, *Nano Lett.*, 2002, 2, 1149-1155.
34. T. S. Haddad, B. D. Viers and S. H. Phillips, *J. Inorg. Organomet. Polym.*, 2001, 11, 155-164.
35. H. G. Jeon, P. T. Mather and T. S. Haddad, *Polym. Int.*, 2000, 49, 453-457.
36. Y. Kim, K. Koh, M. F. Roll, R. M. Laine and A. J. Matzger, *Macromolecules*, 2010, 43, 6995-7000.
37. Y. Peng, T. Ben, J. Xu, M. Xue, X. Jing, F. Deng, S. Qiu and G. Zhu, *Dalton Trans.*, 2011, 40, 2720-2724.
38. W. Chaikittisilp, A. Sugawara, A. Shimojima and T. Okubo, *Chem. Mater.*, 2010, 22, 4841-4843.
39. F. Alves, P. Scholder and I. Nischang, *ACS Appl. Mater. Interfaces*, 2013, 5, 2517-2526.
40. O. Delgado-Friedrichs, M. O'Keeffe and O. M. Yaghi, *Acta Crystallographica Section A*, 2006, 62, 350-355.
41. S. L. Mayo, B. D. Olafson and W. A. Goddard, *J. Phys. Chem.*, 1990, 94, 8897-8909.
42. V. Buch, *J. Chem. Phys.*, 1994, 100, 7610-7629.
43. A. Gupta, S. Chempath, M. J. Sanborn, L. A. Clark and R. Q. Snurr, *Mol. Simul.*, 2003, 29, 29-46.
44. D. Y. Peng and D. B. Robinson, *Industrial and Engineering Chemistry Fundamentals*, 1976, 15, 59-64.
45. O. Talu and A. L. Myers, *AIChE J.*, 2001, 47, 1160-1168.
46. X. D. Li, H. Zhang, Y. J. Tang and X. L. Cheng, *Phys. Chem. Chem. Phys.*, 2012, 14, 2391-2398.
47. R. Q. Snurr, A. T. Bell and D. N. Theodorou, *J. Phys. Chem.*, 1993, 97, 13742-13752.
48. T. Ben, H. Ren, S. Ma, D. Cao, J. Lan, X. Jing, W. Wang, J. Xu, F. Deng, J. M. Simmons, S. Qiu and G. Zhu, *Angewandte Chemie International Edition*, 2009, 48, 9457-9460.
49. H. Frost, T. Duren and R. Q. Snurr, *J. Phys. Chem. B*, 2006, 110, 9565-9570.
50. H. Furukawa, N. Ko, Y. B. Go, N. Aratani, S. B. Choi, E. Choi, A. O. Yazaydin, R. Q. Snurr, M. O'Keeffe, J. Kim and O. M. Yaghi, *Science*, 2010, 329, 424-428.
51. S. S. Han, H. Furukawa, O. M. Yaghi and W. A. Goddard, *J. Am. Chem. Soc.*, 2008, 130, 11580-11581.
52. E. Klontzas, E. Tylianakis and G. E. Froudakis, *J. Phys. Chem. C*, 2008, 112, 9095-9098.
53. J. Palgunadi, H. S. Kim, J. M. Lee and S. Jung, *Chemical Engineering and Processing: Process Intensification*, 2010, 49, 192-198.
54. L. Zhou and Y. P. Zhou, *Industrial and Engineering Chemistry Research*, 1996, 35, 4166-4168.
55. http://www1.eere.energy.gov/hydrogenandfuelcells/mypp/.

Figure captions

Table 1 The LJ potential parameters of H_2, He molecules and all the framework atoms used in the present work.

Table 2 Unit cell parameters, chemical formula, molar mass (M), density, pore volume (V_p), H_2 accessible surface (S), and isosteric heat of adsorption for H_2 molecule of four sil-COFs.

Figure 1 The design scheme of tetraphenyl silsesquioxane based covalent organic frameworks (sil-COFs) with ctn and bor net topology structures.

Figure 2 The comparison of the simulated absolute H_2 adsorption isotherm in COF-102 at 77 K with experimental data by Furukawa et al.[20] and other simulated results by Han et al.[51] and Klontzas et al.[52] with different methods or parameters.

Figure 3 The computed absolute (abs) and excess (exc) H_2 adsorption isotherms in four sil-COFs at 77 K. (a) gravimetric H_2 adsorption isotherms and (b) volumetric H_2 adsorption isotherms.

Figure 4 The computed absolute (abs) and excess (exc) H_2 adsorption isotherms in four sil-COFs at 298 K. (a) gravimetric H_2 adsorption isotherms and (b) volumetric H_2 adsorption isotherms.

Figure 5 The equilibrium snapshots of four sil-COFs structure with H_2 molecules adsorbed under the pressure of 100 bar at 77 K. (a) sil-COF-1, (b) sil-COF-2, (c) sil-COF-3 and (d) sil-COF-4.

Figure 6 The schemes to synthesize the four sil-COFs based on the tetrahedral building blocks, tetra(4-dihydroxyborylphenyl)silsesquioxane (TBPS), and the triangular building block, hexahydroxytriphenylene (HHTP). For clarity, some parts of C and D are omitted.

Table 1 The LJ potential parameters of H_2, He molecules and all the framework atoms used in the present work.

	H_2	He	C	H	O	B	Si
σ(Å)	2.956	2.64	3.473	2.846	3.033	3.581	3.804
ε/k_B (K)	36.7	10.9	47.856	7.649	48.156	47.806	155.997

Table 2 Unit cell parameters, chemical formula, molar mass (*M*), density, pore volume (V_p), H_2 accessible surface (*S*), and isosteric heat of adsorption for H_2 molecule of four sil-COFs.

materials	a=b=c (Å)	chemical formula	*M* (g/mol)	density (g/cm^3)	V_p (cm^3/g)	*S* (m^2/g)	Q_{st} (kJ/mol)	
							77K	298K
sil-COF-1	33.47	$C_{288}H_{192}B_{48}O_{120}Si_{48}$	7439.57	0.33	2.72	5482.92	3.72	4.28
sil-COF-2	21.68	$C_{72}H_{48}B_{12}O_{30}Si_{12}$	1859.89	0.30	2.98	5476.04	3.63	4.18
sil-COF-3	49.52	$C_{576}H_{288}B_{48}O_{168}O_{48}$	11763.45	0.16	5.90	6331.34	2.71	3.47
sil-COF-4	32.22	$C_{144}H_{72}B_{12}O_{42}Si_{12}$	2940.86	0.15	6.54	6323.90	2.72	3.33

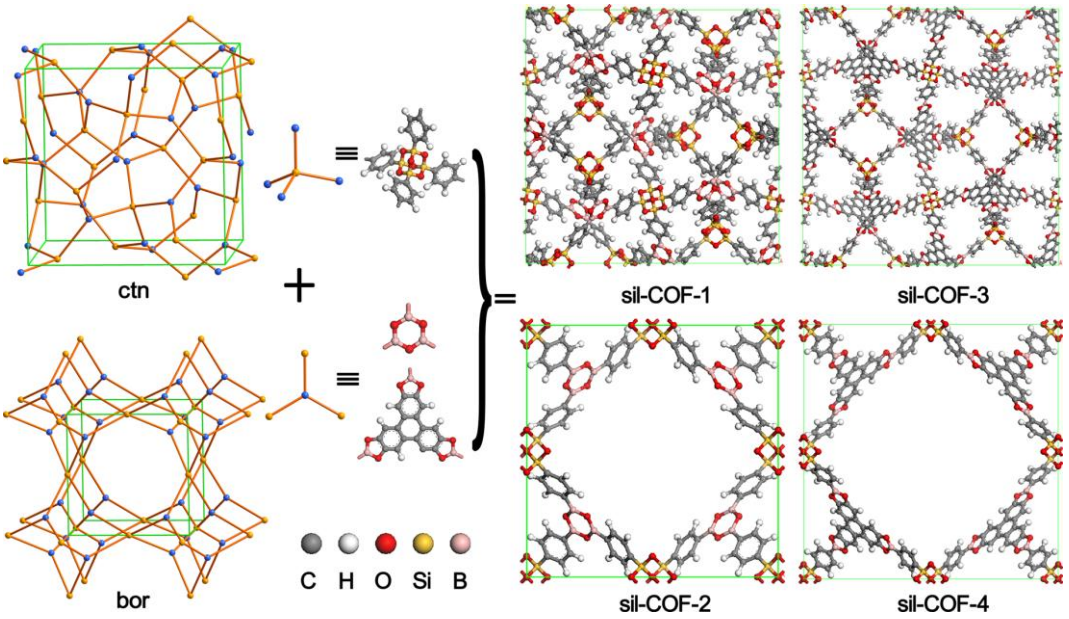

Figure 1 The design scheme of tetraphenyl silsesquioxane based covalent organic frameworks (sil-COFs) with ctn and bor net topology structures.

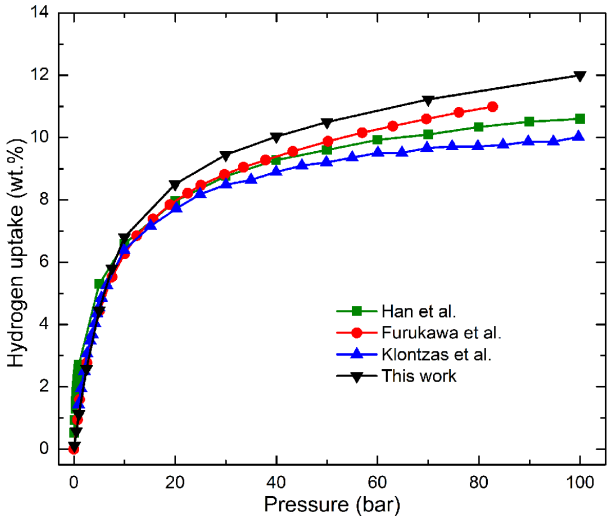

Figure 2 The comparison of the simulated absolute H_2 adsorption isotherm in COF-102 at 77 K with experimental data by Furukawa et al.[20] and other simulated results by Han et al.[51] and Klontzas et al.[52] with different methods or parameters.

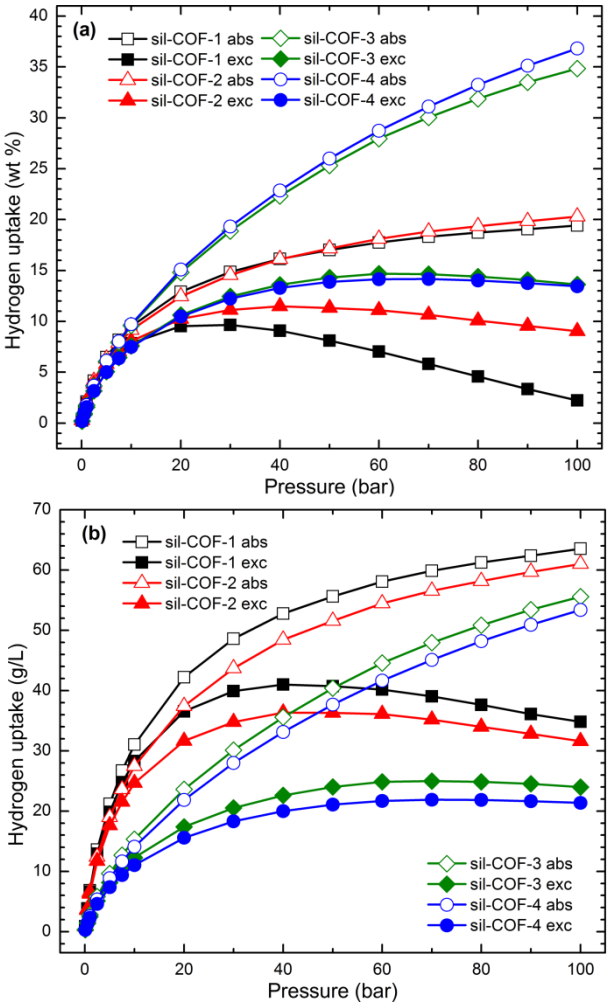

Figure 3 The computed absolute (abs) and excess (exc) H_2 adsorption isotherms in four sil-COFs at 77 K. (a) gravimetric H_2 adsorption isotherms and (b) volumetric H_2 adsorption isotherms.

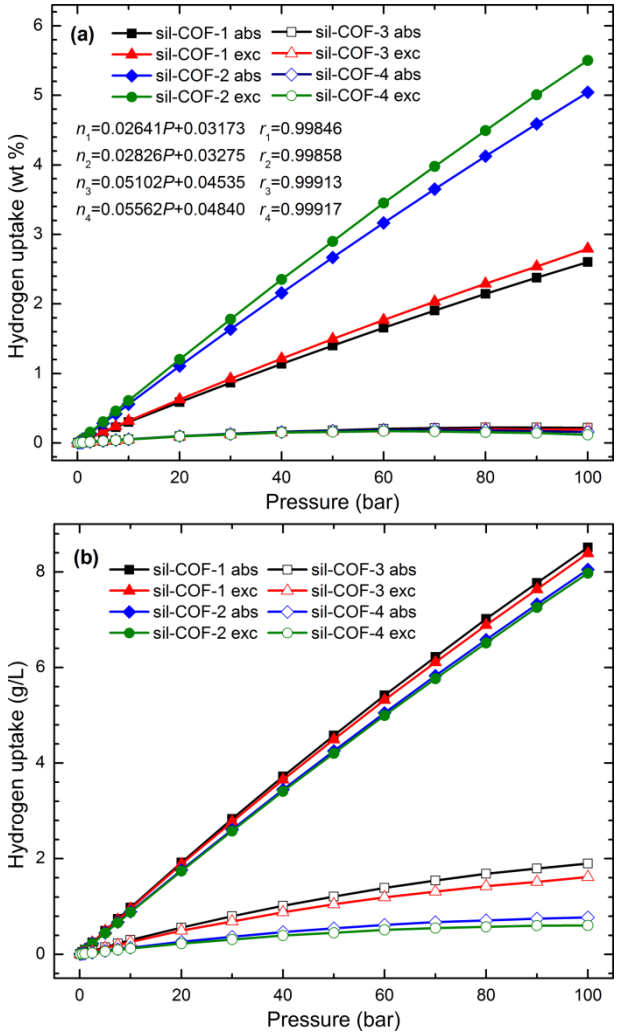

Figure 4 The computed absolute (abs) and excess (exc) H_2 adsorption isotherms in four sil-COFs at 298 K. (a) gravimetric H_2 adsorption isotherms and (b) volumetric H_2 adsorption isotherms.

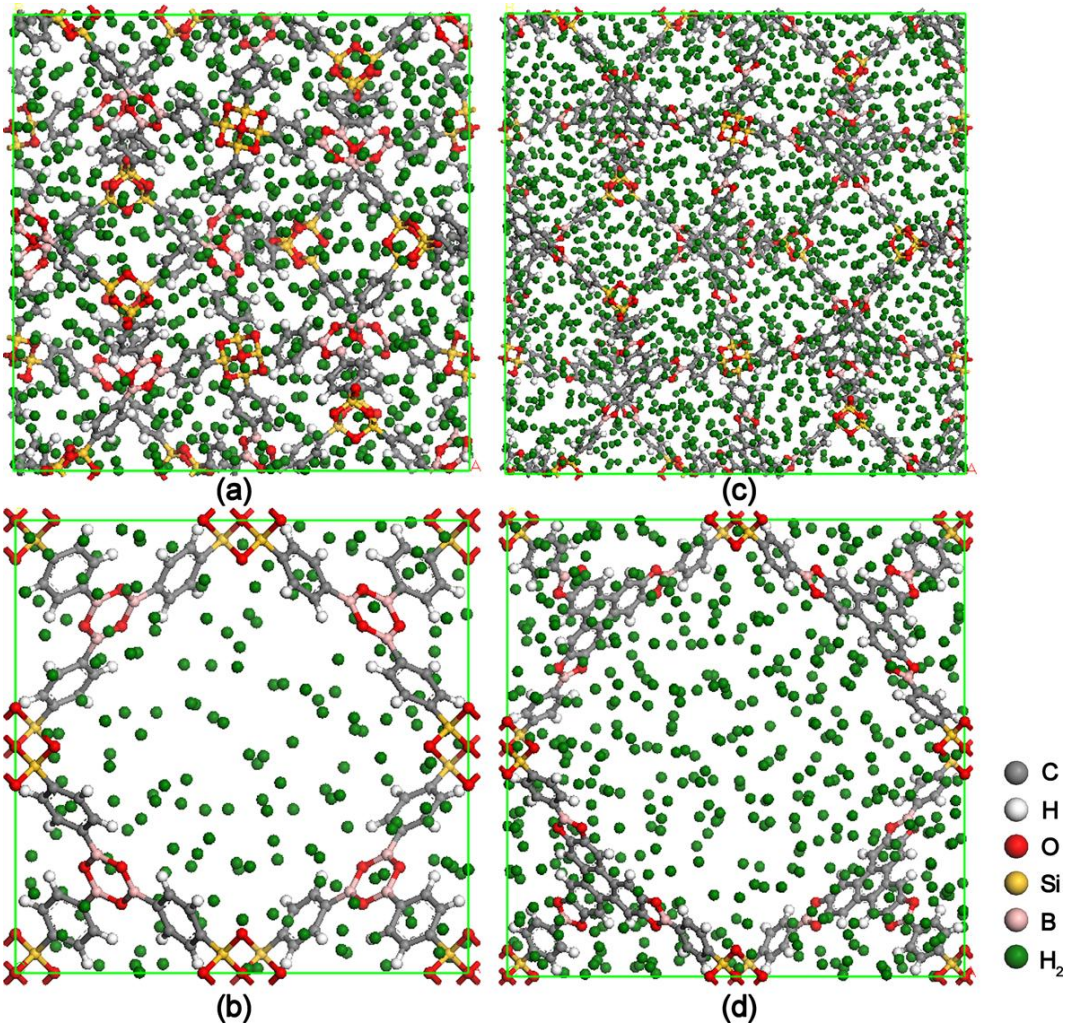

Figure 5 The equilibrium snapshots of four sil-COFs structure with H_2 molecules adsorbed under the pressure of 100 bar at 77 K. (a) sil-COF-1, (b) sil-COF-2, (c) sil-COF-3 and (d) sil-COF-4.

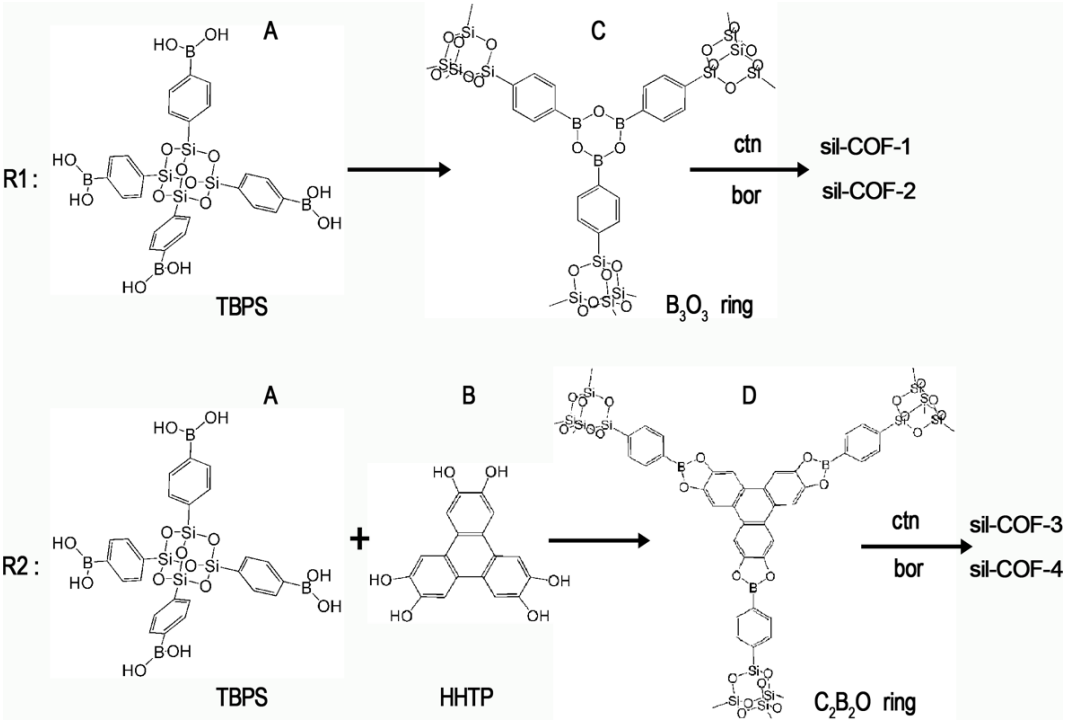

Figure 6 The schemes to synthesize the four sil-COFs based on the tetrahedral building blocks, tetra(4-dihydroxyborylphenyl)silsesquioxane (TBPS), and the triangular building block, hexahydroxytriphenylene (HHTP). For clarity, some parts of C and D are omitted.

Graphical Abstract

Four tetraphenyl silsesquioxane based covalent-organic frameworks (sil-COFs) have been designed under ctn or bor net topology as high-capacity hydrogen storage materials.